Research Square

Preprints are preliminary reports that have not undergone peer review.
They should not be considered conclusive, used to inform clinical practice,
or referenced by the media as validated information.

Leucine-rich repeat kinase 2 negatively regulates glucose tolerance via regulation of membrane translocation of Glucose transporter type 4 in adipocytes

Fumitaka Kawakami (kawakami@kitasato-u.ac.jp)
Kitasato University
Motoki Imai
Kitasato University
Yuki Isaka
Kitasato University
Mark Cookson
National Institutes of Health
Hiroko Maruyama
Kitasato University
Makoto Kubo
Kitasato University
Matthew J. Farrer
University of Florida
Makoto Kanzaki
Tohoku University
Shun Tamaki
Kitasato University
Rei Kawashima
Kitasato University
Tatsunori Maekawa
Kitasato University
Yoshifumi Kurosaki
Kitasato University
Fumiaki Kojima
Kitasato University
Takafumi Ichikawa
Kitasato University

Article

Keywords:

Posted Date: October 28th, 2022

DOI: https://doi.org/10.21203/rs.3.rs-2184589/v1

License: This work is licensed under a Creative Commons Attribution 4.0 International License.
Read Full License

Abstract

Epidemiological studies have shown that abnormalities of glucose metabolism are involved in *leucine-rich repeat kinase 2* (*LRRK2*)-associated Parkinson's disease (PD). However, the physiological significance of this association is unclear. In the present study, we investigated the effect of the LRRK2 on high-fat diet induced glucose intolerance using Lrrk2-knock-out (Lrrk2-KO) mice. We found for the first time that high-fat (HFD) fed Lrrk2-KO mice display improved glucose tolerance and homeostatic model assessment of insulin resistance compared to their wild type (WT) counterparts. We found that Lrrk2 is highly expressed in adipose tissues compared with to other tissues that are thought to be important in glucose tolerance, including skeletal muscle, liver, and pancreas. Lrrk2 expression and phosphorylation of its kinase substrates Rab8a and Rab10 were significantly elevated after HFD treatment in WT mice. Conversely, treatment with a LRRK2 kinase inhibitor stimulated insulin-dependent membrane translocation of insulin-dependent glucose transporter (GLUT4) in 3T3-L1 adipocytes. We conclude that increased LRRK2 kinase activity in adipose tissue exacerbates glucose intolerance by suppressing Rab8- and Rab10-mediated GLUT4 membrane translocation.

Introduction

Leucine rich-repeat kinase 2 (LRRK2) is a protein kinase involved in the development of autosomal dominant Parkinson's disease (PD) and is the causative gene product of PARK8, which has been identified in 2002 (1, 2). LRRK2 contains, armadillo repeat (ARM), ankyrin repeat (ANK), leucine-rich repeat (LRR), Ras-of-complex (ROC) GTPase, C-terminal of ROC (COR), protein kinase and WD40. LRRK2 is mainly expressed in neuronal cells and immune cells, and it is expected to be a cytosolic protein because it does not contain a transmembrane domain (3–6). However, it has been suggested to be localized to organelle membranes (7, 8) and also known to LRRK2 proteins exist in endoplasmic reticulum, Golgi apparatus, early endosomes, lysosomes, synaptic vesicles, mitochondria and plasma membrane (9, 10). As physiological functions of LRRK2 and biological functions involving LRRK2, neurite outgrowth, apoptosis, autophagy, regulation of cytokine production, membrane transport, etc. have been reported (7, 11).

Recently, Rab GTPase, such as Rab8a and Rab10 has been reported as a novel substrate for LRRK2 (12). These two Rab GTPase plays an important role in insulin-dependent membrane transport of glucose transporter 4 (GLUT4) (13). GLUT4 is encapsulated in a special vesicle called GLUT4 storage vesicles (GSV: GLUT4 storage vesicles) via the trans-Golgi network and transported to the cell membrane by insulin signaling (13). Binding of insulin to its receptor sequentially activates the downstream targets, such as IRS-1, PI3-K, and Akt. Activated Akt induces the membrane transport of GLUT-4, which promotes the glucose uptake in insulin-sensitive tissues (adipose, muscle, and liver) (13). It is also known that AMPK also enhances GLUT4 expression and membrane transport. In adipocyte and muscle cells, when AMPK is activated by adiponectin or exercise stimulation, Rab inhibitor AS160 (Rab-GAP) is inhibited by AMPK-mediated phosphorylation. As a result, Rab8a or Rab10 converts to a GTP-binding active form, and these Rab GTPase induce the membrane transport of GLUT4 vesicle (14, 15). Recently, it was reported

that phosphorylation of AS160 is increased in LRRK2 deficient fibroblasts of aged LRRK2-knockout mice (16). We hypothesize that LRRK2 may regulate membrane transport of GLUT4 via Rab8a and Rab10.

Recently, we reported novel role of LRRK2 in glucose metabolism using dexamethasone (DEX)-induced glucose intolerance model mice. In this report, we found that LRRK2 knockout (KO) mice exhibited suppressed glucose intolerance, even after treatment with DEX (17). The phosphorylation of LRRK2, Rab8a and Rab10 was increased in the adipose tissues of DEX-treated wild-type mice. In addition, inhibition of the LRRK2 kinase activity prevented the DEX-induced inhibition of GLUT4 membrane translocation and glucose uptake in cultured 3T3-L1 adipocytes (17). However, the role of LRRK2 on abnormalities in glucose metabolism caused by lifestyle-related abnormalities such as high-fat diets, rather than drug-induced abnormalities, is unknown. In the present study, we investigated that effect of LRRK2 on the high-fat diet induced glucose intolerance in mice. In addition, it was determined that effect of LRRK2 inhibitor on the glucose uptake and insulin-dependent membrane transportation of GLUT4 in cultured adipocyte.

Materials, And Methods

Animal experiments

Five weeks old C57BL/6J male wild-type mice (WT) and Lrrk2 exon 41-KO mice (KO) [21], were used in this study. Mice were allowed *ad libitum* access to either a normal diet (AIN-93M: 15% kcal from fat) or high-fat diet (HFD-60: 60% kcal from fat) obtained from Oriental Yeast Co., Ltd. Tokyo Japan for 5 months with free access to water. There were therefore six experimental groups - WT-ND (WT mouse fed normal diet), WT-HFD (WT mouse fed high-fat diet), KO-ND (KO mouse fed normal diet), KO-HFD (KO mouse fed high-fat diet). These mice were bred and maintained under an environment of room temperature 22°C, 12 hours light and dark cycle in the SPF breeding room of the Kitasato University School of Medical Hygiene and Animal Experiment Facility, with three animals per cage.

Oral glucose tolerance test (OGTT)

Oral glucose tolerance test (OGTT) was performed at one month, three months and five months after exposure to normal or HFD. After fasting for 16 hours from the day before the OGTT test, blood was collected from the tail vein of the mouse and fasting blood glucose measured using a glucometer (Glutest Neo Alpha) (Sanwa Chemical Institute, Japan). Then, a16% glucose solution was orally administered with a gavage to a dose of 2 g / kg body weight. Blood was collected from the tail vein at 15, 30, 45, 60, 90 and 120 minutes after the administration of glucose and the blood glucose level was measured as above. Glucose tolerance evaluation in OGTT was evaluated by the area under the curve (AUC) from the change in blood glucose concentration after oral administration of 16% glucose.

Additionally, blood was collected separately from the blood glucose level measurement at 0 min (fasting), 30 min, and 60 min at the OGTT into 150 µL of heparin solution as an anticoagulant to a final concentration of 50 µg mL^{-1}. The mixed heparin solution was allowed to stand on ice for 2 hours, then

centrifuged at 3,000 rpm for 5 minutes at 4°C. The collected plasma was cryopreserved at -80°C until used for experiments.

Measurements of serum level of insulin, adiponectin and leptin level in mouse.

We measured insulin, adiponectin and leptin level in mice plasma after 5 months of feeding normal or high-fat diet. Plasma insulin, adiponectin, and leptin levels were measured using Levis mouse insulin ELISA kit (U-type for ND group, T-type for HFD group), mouse/rat high-molecular-weight adiponectin ELISA kit and mouse leptin ELISA kit (FUJIFILM Wako Shibayagi Co., Shibukawa, Japan), respectively, as followed manufacturer's instructions. The homeostatic model assessment of insulin resistance (HOMA-IR) value was calculated using the formula:

HOMA-IR = fasting insulin level (μU / mL) × fasting blood glucose level (mg / dL) / 405

HOMA-IR values of 1.6 or less are normal while values of 2.5 or more indicate insulin resistance. As a unit conversion of insulin concentration, 100 IU / mL = 3.53 mg / mL was used.

Western blotting analysis

Mouse tissue or cultured cell pellets were lysed in RIPA Buffer ((25 mM Tris-HCL (pH 7.5), 150 mM NaCl, 1% NP-40, 1% Sodium Deoxycholate, 0.1% SDS with Halt TM Protease & Phosphatase Inhibitor Cocktail 100x (Thermo scientific) and 0.5M EDTA solution (Thermo scientific)) by sonication. Samples were centrifuged (12,700 rpm, 4 ° C., 15 min), the supernatant collected, mixed in a ratio of 3: 1 with 4 × sample buffer mixed with 25: 1 of NuPAGE® LDS sample Buffer 4x (Thermo scientific) with 8 M dithiothreitol and heated at 100°C for 5 minutes. Protein concentrations were measured using the Pierce 660 nm Protein Assay Reagent (Thermo scientific). Proteins were resolved by SDS-polyacrylamide gel electrophoresis using 5–20% acrylamide gradient gels (ATTO). Separated proteins in the gel were transferred to a PVDF membrane (Merk Millipore) using a Trans-Blot Turbo Transfer System (BIO-RAD) and blocked with PVDF Blocking Reagent (TOYOBO, Japan). After overnight incubation at 4°C with primary antibody diluted with Can Get Signal® solution 1 (Toyobo Co., Ltd. Japan), blots were washed 3 times with TBS-T. Blots were then incubated with horseradish peroxidase-conjugated or fluorescence-conjugated secondary antibody diluted with Can Get Signal® solution 2 (Toyobo Co., Ltd. Japan) for 1 h at room temperature. Membranes were washed again 3 times with TBS-T and bands visualized using enhanced chemiluminescence (Pierce ECL Plus Substrate, Thermo scientific) or detected by fluorescence imaging with an ODYSSEY imaging system (LI-COR, USA). To normalize the signal of phospho-specific antibodies to the target protein, blots were stripped by incubating the blot with stripping buffer (62.5 mM Tris-HCl pH 6.8, 2% SDS, and 100 mM β-mercaptoethanol) for 30 min at 70°C, followed by wash steps with TBS-T. Blots were then incubated with an antibody against the total target protein. Band signals were quantitatively analyzed with Image Studio software (LI-COR, USA) as described previously (17).

Antibodies against the following proteins were used: GLUT-4 (2213S; Cell Signaling Technology, 1:1000), AKT (9272S; Cell Signaling Technology, 1:2000), P-AKT(S473, 4051S; Cell Signaling Technology, 1:1000), AMPK (2793S; Cell Signaling Technology, 1:2000), P-AMPK (T172, 2531S; Cell Signaling Technology,

1:1000), LRRK2 (ab033474; Abcam, 1:2000), P-LRRK2 (S935, ab133450; Abcam, 1:1000), Rab8a (ab237702; Abcam, 1:4000), P-Rab8a (T72, ab230260; Abcam, 1:1000), Rab10 (ab237703, abcam, 1:4000), P-Rab10 (T73, ab23026; Abcam, 1:1000), AS160 (ABV10742, ABGENT, 1:2000), P-AS160 (PA080083, CUSABIO, 1:1000), β-Actin (5125S; Cell Signaling Technology, 1:5000) and GAPDH (3683S; Cell Signaling Technology, 1:5000). The secondary antibodies were HRP donkey anti-mouse IgG (H + L) antibody (1:5000) and HRP donkey anti-rabbit IgG (H + L) antibody (Biolegend) all at a dilution of 1:5,000.

3T3-L1 cell culture and differentiation to adipocyte

3T3-L1 cells were cultured in low glucose (1g L^{-1}) Dulbecco's modified Eagle's medium (DMEM) containing 10% calf serum and 5% (v/v) penicillin and streptomycin sulfate in a humidified atmosphere of 5% CO_2 at 37°C. For differentiation to adipocytes, cells were seeded plates or coverslip with high glucose (4500 mg L^{-1}) DMEM and 10% FBS with media change every 2–3 days until confluency reached 70%. Subsequently, cells were treated with 0.1% dexamethasone, 1% isobutyl methylxanthine, IBMX and 0.1% bovine insulin in DMEM containing 10% FBS for two days without medium change then 0.1% insulin-containing fresh DMEM containing 10% FBS for the next 2 days. Thereafter, cells were maintained in insulin-free DMEM with 10% FBS till the cells were completely differentiated into adipocytes (8 days after initiation) as described previously (17, 18).

Immunofluorescent cytochemistry (ICC)

Myc-GLUT4-ECFP stably expressing 3T3-L1 (3T3-L1-G4) cells were cultured and differentiated in 24 well culture plates on Poly D-lysine/Laminin coated coverslips as described previously (17, 18). Cells were fixed in 4% paraformaldehyde in PBS and nonspecific immunoreactivity blocked using 1% BSA in PBS. Primary antibody solution (anti-myc mouse monoclonal IgG in blocking solution; 1:300 dilution) was added to wells and incubated overnight at 4°C. After washing, secondary antibody (Alexa 594 labeled anti-mouse IgG) was used to detect the myc epitope of myc-GLUT4-ECFP located at the cell surface. After subsequent washing and mounting, a confocal fluorescence microscope was used to visualize stained cells.

Glucose cellular uptake measurement in 3T3-L1 cell

Glucose uptake in 3T3-L1 cells was measured using a Glucose cellular uptake measurement kit (COSMO bio Co., LTD) as described in manufacturer's instructions. Briefly, differentiated 3T3-L1 cells seeded on 12 well plates were treated with LRRK2 inhibitors (1–2 μM CZC25146 or 0.1–0.2 μM MLi-2) for 6 h. After culture medium was removed, cells were incubated in serum free medium for 6h, washed with Krebs Ringer Phosphate Hepes (KRPH) buffer alone then KRPH buffer containing 2% BSA. After stimulating the cells with 200 nM insulin, 2-deoxy glucose solution was added to 1 mM and incubated for 10 min. Then, cells were washed by cold PBS, and cells were collected with sample diluent buffer and immediately sonicated. Cell lysates were heated at 80 ° C for 15 minutes then immediately centrifuged (15,000xg, 20 minutes). Supernatants were mixed with reaction solution containing fluorescent substrate and enzyme (diaphorase) in a 96-well black plate, and incubated at 37 ° C for 2 hours in the dark. The fluorescence intensity of sample was measured by a fluorescence plate reader.

Data analysis

In animal experiments, data represent the mean ± standard error of the mean (SEM). In biochemical analysis, data represent the mean ± standard deviation (SD) of one of the three independent experiments each performed in triplicate. Data analysis and curve fitting were performed with GraphPad Prism 6.0 (GraphPad Software).

Study approval

The animal experimental protocol was approved by the Animal Care and Use Committee (Approval number Eiken-ken 18–56) and Genetic Modification Experiment Safety Committee (Approval number 3952) of the Kitasato University in agreement with accepted international standards, and followed the recommendations in the ARRIVE guidelines. The all experiments were performed in accordance with the relevant guidelines and regulation.

Results

1. LRRK2 deficiency is associated with lower weight gain after high fat diet.

Lrrk2-KO mice gained significantly less weight than their WT counterparts after 10 weeks of access to a high fat diet, whereas no significant differences were observed between genotypes on normal diet (Supplemental fig. S1 A and B). This did not appear to be due to differences in food consumption between genotype, as Lrrk2-KO mice had higher intake than WT animals during some weeks in both normal and high-fat food fed conditions (Supplemental fig. S1 A and B). However, the weight of liver, perirenal and epididymal adipose tissue of Lrrk2-KO mice were significantly lower than WT after exposure to high fat diet (Supplemental fig. S1 C and D). These results suggest that endogenous LRRK2 normally depresses the responsiveness of insulin-sensitive tissues to high fat diet-induced weight gain *in vivo*.

2. LRRK2 knockout mice display improved glucose intolerance by high fat diet.

Based on these observations, we postulated that Lrrk2-knockout animals would show altered insulin responses, of which glucose tolerance is a widely used outcome measure. We therefore performed OGTT at 1, 3 and 5 months from the start of feeding normal or high fat diets in wild type and Lrrk2-KOmice. In the ND group, the serum glucose level of Lrrk2-KO mice after oral glucose was significantly lower than WT mice at each months (Fig. 1A and Supplemental Fig. S2 A and B). After one month of HFD, the serum glucose level of Lrrk2-KO mice at the 15, 90 and 120 min of OGTT time points was significantly lower than WT (Supplemental Fig. S1 A). Furthermore, after 3 months of HFD, serum glucose was significantly lower in Lrrk2-KO mice compared to WT at many timepoints tested (Supplemental Fig. S1 B). In HFD 5 month group, serum glucose level of Lrrk2-KO mice is also significantly lower than WT mice (Fig. 1B). We also investigated the glucose tolerance of these mice using AUC values. Although there were no differences in normal diet, AUC of Lrrk2-KO mice was significantly lower than that of WT at 1, 3 and 5 months of high fat diet (Fig. 1C and Supplemental Fig. S2 C and D).

3. LRRK2 deficiency ameliorate insulin resistance induced by high fat diet.

Next, we determined serum insulin levels after five months of exposure to normal or high fat diets. Fasting serum insulin level of HFD fed mice was 20 to 100-fold higher than the normal diet group (Fig. 2A and B), confirming the expected hyperinsulinemia in our experimental condition. However, although no significant differences in insulin levels were noted under normal diet (Fig. 2A), the insulin level of HFD fed Lrrk2-KO mice at baseline and at 30 min of OGTT was significantly lower than WT (Fig. 2B). Furthermore, we evaluated HOMA-IR as a point measure of insulin resistance and found that HOMA-IR of HFD-fed Lrrk2-KO mice was significantly lower than WT (Fig. 2C).

4. Comparison of serum high molecular weight adiponectin (HMW-Adiponectin) and leptin level of ND- or HFD-fed WT and KO mice.

It is well known that glucose intolerance associated with high-fat feeding leads to decreased high molecular weight (HMW) adiponectin and increased serum levels of leptin. We therefore assessed these markers in WT and Lrrk2-KO mice. We found that HMW Adiponectin level was significantly decreased by high fat diet feeding in wild type mice, but that there were no significant changes in Lrrk2-KO mice (Fig. 3A). Serum leptin levels were increased in both WT and Lrrk2-KO mice fed HFD compared with ND but to a significantly lower extent in the HFD-fed Lrrk2-KO animals (Fig. 3B). These biochemical assays support a diminished response to high fat diet in Lrrk2-animals that correlates with lower insulin levels after OGTT.

5. Determination of phosphorylation and expression of LRRK2 and insulin signaling-related molecules in the adipose tissue of ND- or HFD-fed WT and KO mice.

The above results indicate that KO mice have improved glucose tolerance and insulin resistance after exposure to a high-fat diet, suggesting that LRRK2 may play an important role in glucose metabolism. However, this does not establish LRRK2 plays a direct role in insulin signaling within tissues or cells. Therefore, we investigated LRRK2 protein expression in insulin-sensitive tissues, such as adipose, skeletal muscle, and liver in WT mice. Lrrk2 was highly expressed in adipose tissue, although slightly lower than in brain, while it was difficult to detect in muscle and liver. (Fig. 4). These results suggest that if LRRK2 is involved in the whole animal response to HFD then this is likely via effects on adipose tissue.

Next, we determined the effect of HFD on LRRK2 expression and kinase activity in adipose tissue. Rab8a and Rab10 are reported to be substrates for LRRK2, and are also known to be important molecules for insulin signaling (37). Therefore, we analyzed phosphorylation of Rab8a and Rab10 as an indicator for LRRK2 kinase activity. Strikingly, we found that the expression of LRRK2 in adipose tissue was significantly increased in high-fat-fed WT mice (Fig. 5A). The same antibody gave no signal in Lrrk2-KO mice, validating the utility of this reagent for evaluation of endogenous LRRK2. Additionally, phosphorylation of Rab8a and Rab10 were both significantly increased in high-fat-fed WT mice, whereas LRRK2 phosphorylation was not significantly changed (Fig. 5B—D). These results show that the endogenous expression and activity of LRRK2 are increased by chronic HFD *in vivo*.

Next, we investigated the expression of GLUT4 and expression or phosphorylation of AS160, Akt and AMPK in adipose tissue of these mice by western blotting. We found that phosphorylation of AS160 was significantly decreased in HFD fed WT mice compared with ND fed WT mice (Fig. 5E). However, no significant difference was observed in expression and phosphorylation of GLUT4, Akt and AMPK (Fig. 5F—J). These results suggested that LRRK2 kinase activity may not have a direct effect on these molecules in insulin signaling.

6. LRRK2 kinase inhibition promotes GLUT4 membrane translocation in 3T3-L1 adipocytes.

Although the above results did not support a role of LRRK2 in the overall levels of GLUT4 in tissue, GLUT4 activity is also influenced by trafficking to the cellular membrane. To assess any potential effect of LRRK2 kinase activity on GLUT4 membrane translocation, we used myc-GLUT4-ECFP stably expressing 3T3-L1 adipocyte (3T3-L1-G4). This GLUT4 possesses the c-myc epitope tag in the first extracellular loop and Enhanced Cyan Fluorescent Protein (ECFP) at the c-terminus, allowing us to detect the extracellular domain of GLUT4 translocated to the plasma membrane by immunostaining for myc tag without membrane permealization.

Differentiated 3T3-L1-G4 cells were stimulated by Insulin in the presence or absence of two structurally distinct LRRK2 kinase inhibitors, CZC25146 and MLi-2. As expected, while there was no signal in the absence of insulin fluorescence intensity of myc staining was increased by insulin stimulation (Fig. 6A, B and E). Fluorescence intensity at plasma membrane was potently increased by the addition of both LRRK2 kinase inhibitors in the presence of insulin (Fig. 6C, D and E). Further supporting these observations, we also found that the same LRRK2 kinase inhibitors significantly promoted insulin-dependent glucose uptake in the normal 3T3-L1 cells (Fig. 6F). Phosphorylation of Lrrk2, Rab8a, and Rab10 were also significantly decreased under the same conditions of LRRK2 inhibition (Fig. 7B—D), whereas no effect on the Lrrk2 expression was observed (Fig. 7A). These results suggest that LRRK2 kinase activity negatively regulates GLUT4 membrane translocation in adipocytes, likely via Rab8a and Rab10 phosphorylation.

Discussion

In the present study, we investigated the effect of LRRK2 on the regulation of blood glucose level using a glucose intolerance model with a high-fat diet. We found that deterioration of glucose tolerance after feeding with high-fat diet was significantly suppressed in Lrrk2-KO mice. Furthermore, Lrrk2-KO mice had lower serum insulin level and improvement of HOMAR-IR compared with WT mice with high-fat diet. Our findings identify a new physiological role of LRRK2 that regulates glucose metabolism *in vivo*.

To understand the mechanism of LRRK2-mediated regulation of blood glucose level, we determined the expression of LRRK2 protein in insulin-related tissues. We found Lrrk2 highly expressed in the adipose tissue among insulin-related tissues such as pancreas, skeletal muscle, and liver. adipose tissue is highly insulin-responsive and plays a central role in regulation of the whole-body energy and glucose homeostasis. It is also known that adipose tissue is an active endocrine organ, secreting various

hormones, such as adiponectin and leptin. In obesity, increased leptin and decreased adiponectin serum level have been reported to correlate with insulin resistance and type-2 diabetes. Therefore, we evaluated the serum leptin and adiponectin level between WT mice and Lrrk2-KO mice fed a normal or high-fat diet. While adiponectin was significantly decreased by high-fat diet in WT mice, this was not seen in Lrrk2-KO mice. In contrast, leptin was significantly lower in Lrrk2-KO mice than WT mice despite the increase in serum level in both WT and Lrrk2-KO mice due to high-fat diet. However, there was no difference in adipocytokine secretion between WT and Lrrk2-KO mice under normal diets, suggesting that LRRK2 is involved in regulation of insulin-dependent glucose uptake rather than the adipocytokine secretion.

In adipose tissue, insulin signaling induces glucose uptake by stimulation of membrane-translocation of the insulin-dependent glucose transporter GLUT4 (13). Activation of Akt and AMPK signaling enhances the expression and membrane translation of GLUT4 by phosphorylation-mediated inhibition of AS160 Rab GAP, which is an inhibitor for Rab8a and Rab10 on GLUT4 vesicles (13). As these Rab GTPases are kinase substrates for LRRK2 (12), we determined expression and phosphorylation of Lrrk2, Rab8a, Rab10, and insulin signaling molecules such as GLUT4, AS160, Akt and AMPK. Strikingly, we found that Lrrk2 expression was significantly increased in adipose tissue of high-fat diet fed WT mice and also that phosphorylation of Rab8a and Rab10 were significantly increased in adipose tissue of high-fat diet fed WT mice but not in Lrrk2-KO mice.

Previous reports have shown that LRRK2 phosphorylates conserved residues located on the switch II domain that play a role in GDP / GTP conversion and interaction with Rab effector proteins (18), and phosphorylation of Rab by LRRK2 on its domain causes each Rab to convert to the inactive GDP bound form (18). In addition, the GTP/GDP bound state of Rabs is regulated by inherent GTPase (19). However, inherent Rab GTPase activity is typically insufficient for activation of GTPase activity and hence Rab-specific GTPase-activating protein (GAP) are required activation (19). AS160 is the Rab GTPase-activating protein known to active against Rabs 2A, 8A, 10 and 14, and regulates GLUT4 trafficking in adipocytes (20). Previously, AS160 is reported to be phosphorylated by Akt and AMPK after insulin stimulation (20). Nonphosphorylated AS160 binds to GLUT4 vesicles and inhibits GLUT4 translocation, and phosphorylation of AS160 overcomes this inhibitory effect (20). Thus, phosphorylation of AS160 in adipocytes is required for insulin-stimulated translocation of GLUT4 to the plasma membrane. Here, we found that phosphorylation of AS160 in adipose tissue was significantly decreased by high-fat diet in WT mice but not Lrrk2-KO mice. In insulin resistant adipose tissue induced by high-fat diet, Akt activity is suppressed and, as a result, there is a decrease of AS160 phosphorylation and upregulation of Rab GAP activity of AS160. Therefore, our results suggests that increased phosphorylation of Rab8a and Rab10 due to enhanced LRRK2 expression and decrease of AS160 phosphorylation, caused by high-fat diet intake may synergistically downregulate GLUT4 membrane translocation in adipose tissue.

To confirm the suppressing effect of LRRK2 on the GLUT4 membrane translocation at cellular level, we performed immunofluorescence analysis of GLUT4 using Myc-GLUT4-ECFP stably expressing 3T3-L1 adipocyte. By examining translocation to plasma membrane after insulin stimulation, it was found that both two structurally distinct LRRK2 kinase inhibitors (CZC25146 and MLi-2) robustly promoted the

membrane translocation of GLUT4. Furthermore, we found that these two LRRK2 inhibitors significantly increased glucose uptake in the cells. Western blotting analysis showed that these two LRRK2 inhibitors significantly inhibited the phosphorylation of LRRK2 (Ser935), Rab8a (Thr72) and Ranb10 (Thr73) at insulin stimulated conditions. All these results of experiments using cultured adipocyte suggest that LRRK2 kinase activity suppress the insulin-dependent glucose uptake through negative regulation of GLUT4 membrane translocation via induction of the phosphorylation of Rba8a and Rab10 in adipocytes. Thus, we propose that inhibition of the LRRK2 kinase activity targeted to improvement of glucose intolerance may be a new strategy for treatment of glucose metabolism disorders.

It has been reported that abnormalities of glucose metabolism are found in 50 to 80% of PD patients and that about 40% of patients with type-2 diabetes has high risk for developing PD [46–50]. In addition, insulin resistance and pre-diabetic condition are thought to adversely affect PD pathology, especially insulin resistance is known to worsen the pathology of PD and increase the risk of dementia [9–12]. Furthermore, statin therapy, a cholesterol-lowering drug, delays the onset of Parkinson's disease in diabetic patients [13], thus it is suggested that type 2 diabetes and PD may share a common mechanism of pathogenesis. Therefore, our findings suggests that abnormal glucose metabolism caused by LRRK2 activation may be triggered the pathogenesis of PD at early life stage.

Declarations

Acknowledgements

This work was supported in part by a grant from JSPS KAKENHI Grant Number 19K08985.

Data Availability

The data is available from the corresponding author upon reasonable request.

References

1. Funayama, M., Hasegawa, K., Kowa, H., Saito, M., Tsuji, S., & Obata, F. (2002) Ann. Neurol., 51, 296–301.
2. Paisán-Ruíz, C., Jain, S., Evans, E.W., Gilks, W.P., Simón, J., van der Brug, M., López de Munain, A., Aparicio, S., Gil, A.M., Khan, N., Johnson, J., Martinez, J.R., Nicholl, D., Carrera, I.M., Pena, A.S., de Silva, R., Lees, A., Martí-Massó, J.F., Pérez-Tur, J., Wood, N.W., & Singleton, A.B. (2004) Neuron, 44, 595–600.
3. West A.B., Moore D.J., Biskup S., Bugayenko A., Smith W.W., Ross C.A., (2005) Parkinson’s disease-associated mutations in leucine-rich repeat kinase 2 augment kinase activity. Proc. Natl. Acad. Sci. U.S.A. 102, 16842–16847
4. Thévenet J., Pescini Gobert R., Hooft van Huijsduijnen R., Wiessner C., Sagot Y.J. (2011) Regulation of LRRK2 expression points to a functional role in human monocyte maturation. PLoS ONE 6,

e21519

5. Fan Y., Howden A.J., Sarhan A.R., Lis P., Ito G., Martinez T.N., (2017) Interrogating Parkinson's disease LRRK2 kinase pathway activity by assessing Rab10 phosphorylation in human neutrophils. Biochem. J. 475, 23–44
6. Gloeckner C.J., Kinkl N., Schumacher A., Braun R.J., O'Neill E., Meitinger T., (2006) The Parkinson disease causing LRRK2 mutation I2020T is associated with increased kinase activity Hum. Mol. Genet. 15, 2020–232
7. Hatano T., Kubo S.-I., Imai S., Maeda M., Ishikawa K., Mizuno Y., (2007) Leucine-rich repeat kinase 2 associates with lipid rafts. Hum. Mol. Genet. 16, 678–690
8. Ito G., Iwatsubo T. (2012) Re-examination of the dimerization state of leucine-rich repeat kinase 2: predominance of the monomeric form. Biochem. J. 441, 987–994
9. West A. B., Moore D. J., Biskup S., Bugayenko A., Smith W. W., Ross C. A., Dawson V. L. and Dawson T. M. (2005) Parkinson's disease-associated mutations in leucine-rich repeat kinase 2 augment kinase activity. Proc. Natl Acad. Sci. USA 102, 16842–16847.
10. Biskup S., Moore D. J., Celsi F. et al. (2006) Localization of LRRK2 to membranous and vesicular structures in mammalian brain. Ann. Neurol. 60, 557–569.
11. Sakaguchi-Nakashima A., Meir J. Y., Jin Y., Matsumoto K. and Hisamoto N. (2007) LRK-1, a C. elegans PARK8-related kinase, regulates axonal-dendritic polarity of SV proteins. Curr. Biol. 17, 592–598.
12. Steger M., Tonelli F., Ito G., Davies P., Trost M., Vetter M., Wachter S., Lorentzen E., Duddy G., Wilson S., Baptista M.A., Fiske B.K., Fell M.J., Morrow J.A., Reith A.D., Alessi D.R., Mann M. (2016) Phosphoproteomics reveals that Parkinson's disease kinase LRRK2 regulates a subset of Rab GTPases. Elife. 5. pii: e12813.
13. Jaldin-Fincati JR, Pavarotti M, Frendo-Cumbo S, Bilan PJ, Klip A. (2017) Update on GLUT4 Vesicle Traffic: A Cornerstone of Insulin Action. Trends Endocrinol Metab. 8, 597–611
14. Xie B, Chen Q, Chen L, Sheng Y, Wang HY, Chen S. (2016) The Inactivation of RabGAP Function of AS160 Promotes Lysosomal Degradation of GLUT4 and Causes Postprandial Hyperglycemia and Hyperinsulinemia. Diabetes. 65, 3327–3340.
15. Mîinea C.P., Sano H., Kane S., Sano E., Fukuda M., Peränen J., Lane W.S., Lienhard G.E. (2005) AS160, the Akt substrate regulating GLUT4 translocation, has a functional Rab GTPase-activating protein domain. Biochem J. 391, 87–93.
16. Funk N, Munz M, Ott T, Brockmann K, Wenninger-Weinzierl A, Kühn R, Vogt-Weisenhorn D, Giesert F, Wurst W, Gasser T, Biskup S. (2019) The Parkinson's disease-linked Leucine-rich repeat kinase 2 (LRRK2) is required for insulin-stimulated translocation of GLUT4. Sci Rep. 9, 4515.
17. Imai M, Kawakami F, Kubo M, Kanzaki M, Maruyama H, Kawashima R, Maekawa T, Kurosaki Y, Kojima F, Ichikawa T. (2020) LRRK2 Inhibition Ameliorates Dexamethasone-Induced Glucose Intolerance via Prevents Impairment in GLUT4 Membrane Translocation in Adipocytes. Biol Pharm Bull. 43, 1660–1668.

18. Pfeffer SR. (2018) LRRK2 and Rab GTPases. Biochem Soc Trans. 46, 1707–1712.
19. Stenmark H. (2009) Rab GTPases as coordinators of vesicle traffic. Nat Rev Mol Cell Biol. 10, 513–525.
20. Fujita H, Hatakeyama H, Watanabe TM, Sato M, Higuchi H, Kanzaki M. (2010) Identification of three distinct functional sites of insulin-mediated GLUT4 trafficking in adipocytes using quantitative single molecule imaging. Mol Biol Cell. 21, 2721–2731.
21. Hinkle K.M., Yue M., Behrouz B., Dächsel J.C., Lincoln S.J., Bowles E.E., Beevers J.E., Dugger B., Winner B., Prots I., Kent C.B., Nishioka K., Lin W.L., Dickson D.W., Janus C.J., Farrer M.J., Melrose H.L. (2012) LRRK2 knockout mice have an intact dopaminergic system but display alterations in exploratory and motor co-ordination behaviors. Mol. Neurodegener., **7**, 25

Figures

Fig. 1.

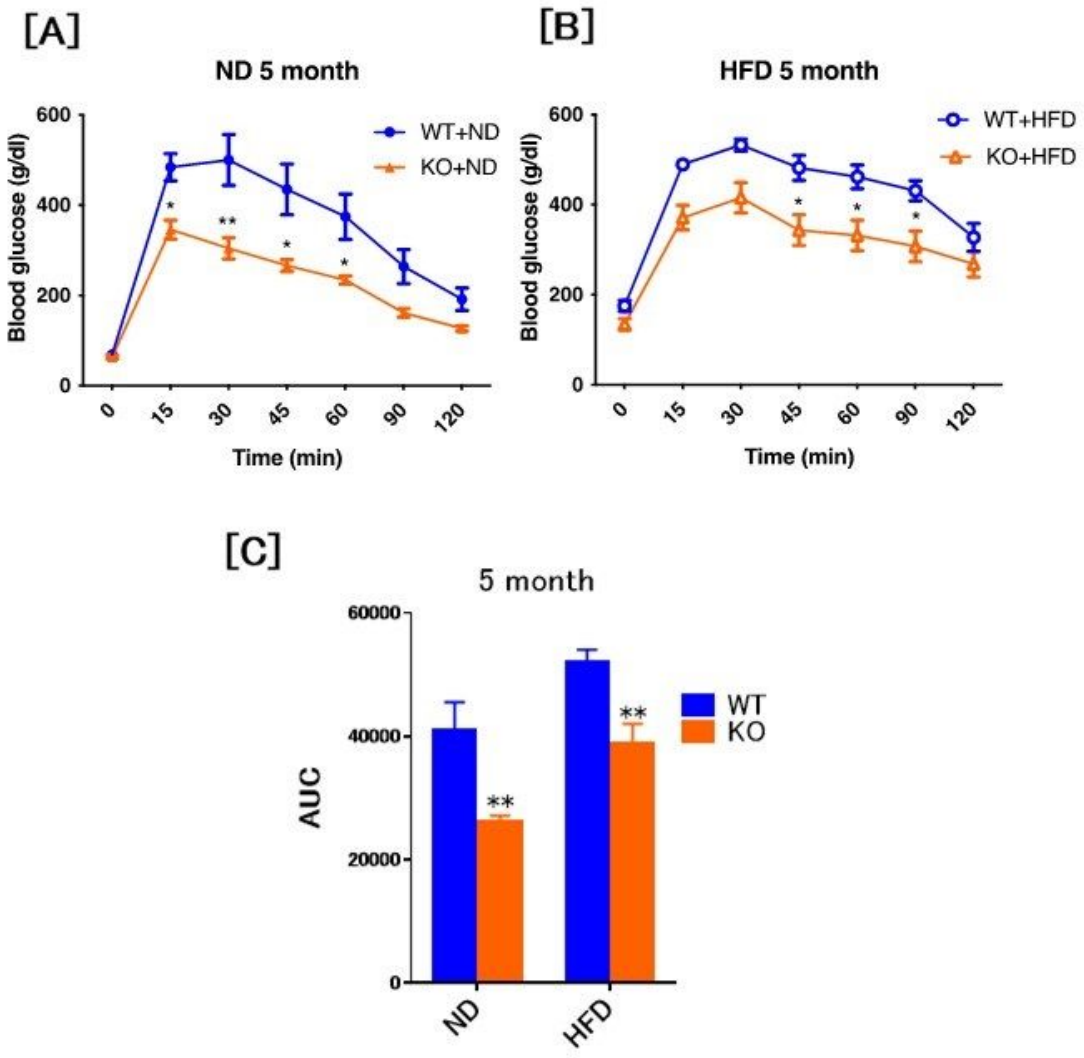

Figure 1

Comparison of blood glucose changes in OGTT of ND- or HFD-fed WT and Lrrk2-KO mice.

Five-week old WT and Lrrk2-KO mice were reared on ND or HFD for 20 weeks. OGTT was performed at 5 months from the start of feeding each diet. Blood glucose variation curve of ND group (A) and HFD group (B) at 5 months are shown with wild type animals in blue and Lrrk2-knockout in red. Area under the curve

(AUC) of OGTT at 5 months (C) were indicated. Data are presented as means ± SEM (n = 9 animals per group). Data of blood glucose variation curve were analyzed by two-way ANOVA combined with Sidak post hoc test. *p<0.05, **p<0.01 (WT vs KO).

Fig. 2.

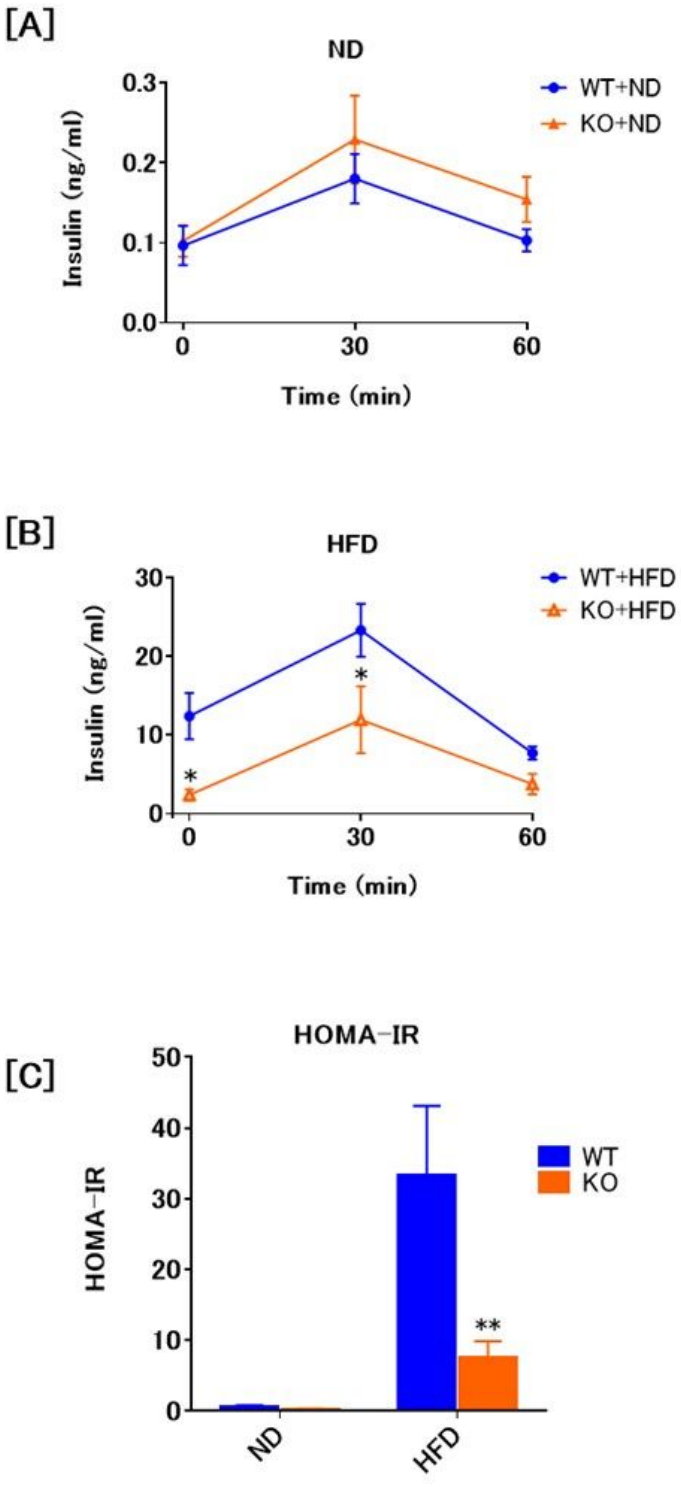

Figure 2

Comparison of serum insulin levels of ND- or HFD-fed WT and Lrrk2-KO mice.

Time course of serum insulin levels at 5 months of ND-fed WT and Lrrk2-KO mice (A) and HFD-fed WT and KO mice (B) were measured by ELISA. Homeostatic model assessment-estimated insulin resistance (HOMA-IR) of ND- or HFD-fed WT and Lrrk2-KO mice at 5 month was indicated in (C). Data are presented as means ± SEM (n = 9 animals per group). The data were analyzed by two-way ANOVA combined with Sidak post hoc test. *p<0.05, **p<0.01 (WT vs KO).

Fig. 3.

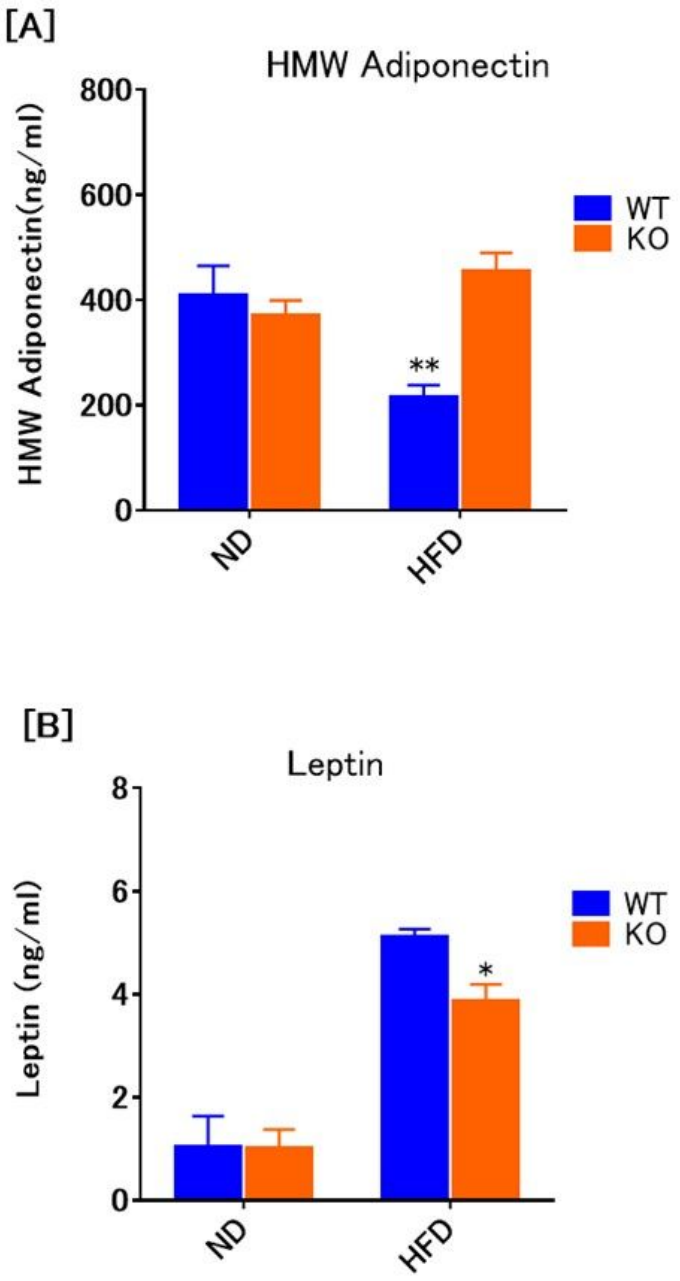

Figure 3

Comparison of serum Adiponectin and Leptin levels of ND- or HFD-fed WT and Lrrk2-KO mice.

Serum Adiponectin and Leptin levels at 5 months of ND-fed WT and Lrrk2-KO mice (A) and HFD-fed WT and Lrrk2-KO mice (B) were measured by ELISA. Data are presented as means ± SEM (n = 9). The data were analyzed by two-way ANOVA combined with Sidak post hoc test. *p<0.05, **p<0.01 (WT vs Lrrk2-KO). N.S., no significance.

Fig. 4.

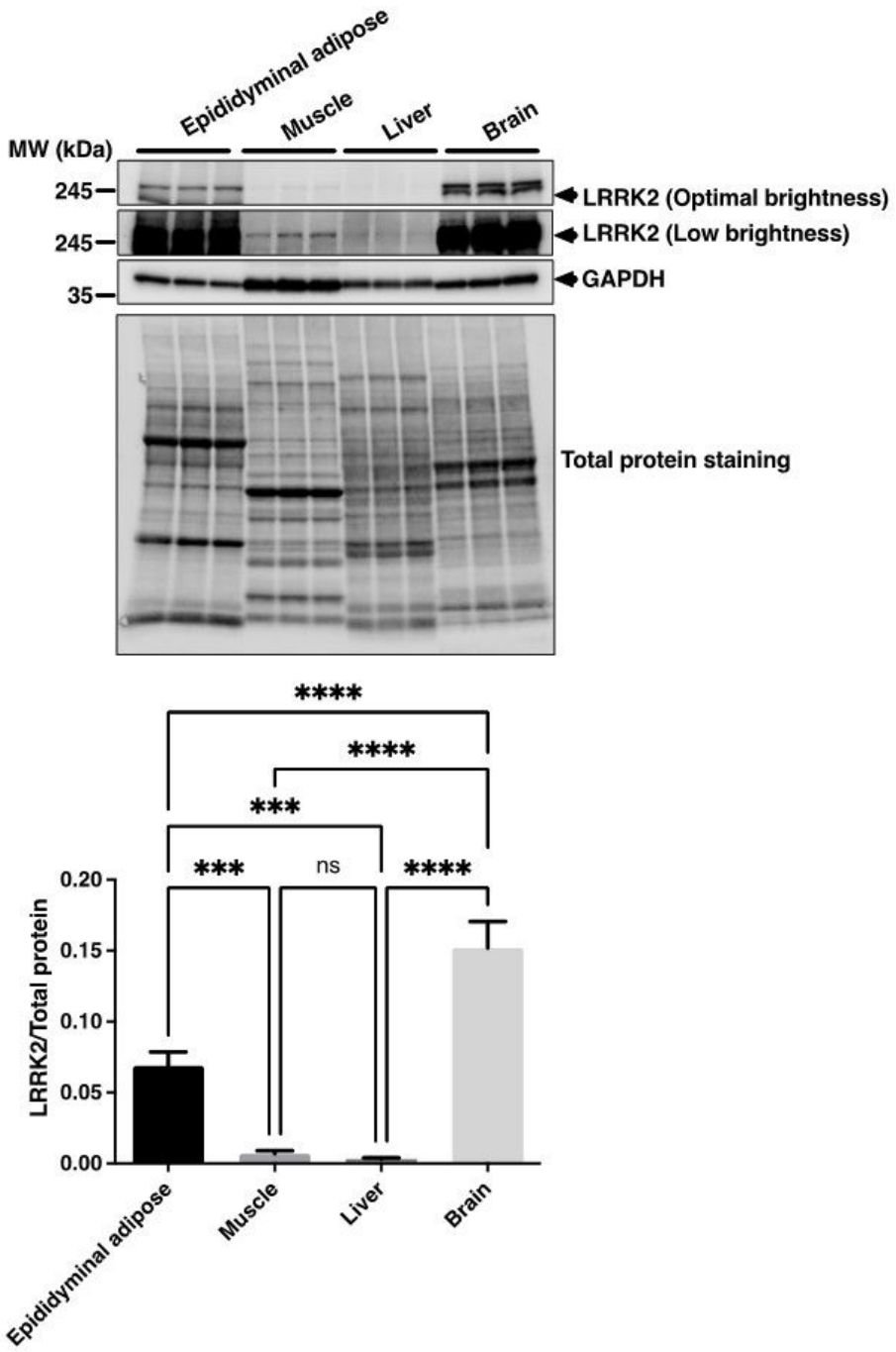

Figure 4

Detection of Lrrk2 protein expression in insulin sensitive tissues of WT mice.

Lrrk2 protein expression in epididymal adipose, skeletal muscle and liver of male WT mice were determined by western blot analysis, as described in Materials and Methods. The brain sample was used as positive control for Lrrk2 protein expression. All protein bands were visualized by chemiluminescence using a LI-COR's Odyssey Fc Dual-Mode Imaging System (LI-COR Biosciences, USA). The band intensity of Lrrk2 was normalized by GAPDH used as loading control. Data are presented as means ± SEM (n = 9). The data were analyzed by one-way ANOVA combined with Tukey's post hoc test. **p<0.01.

Fig. 5.

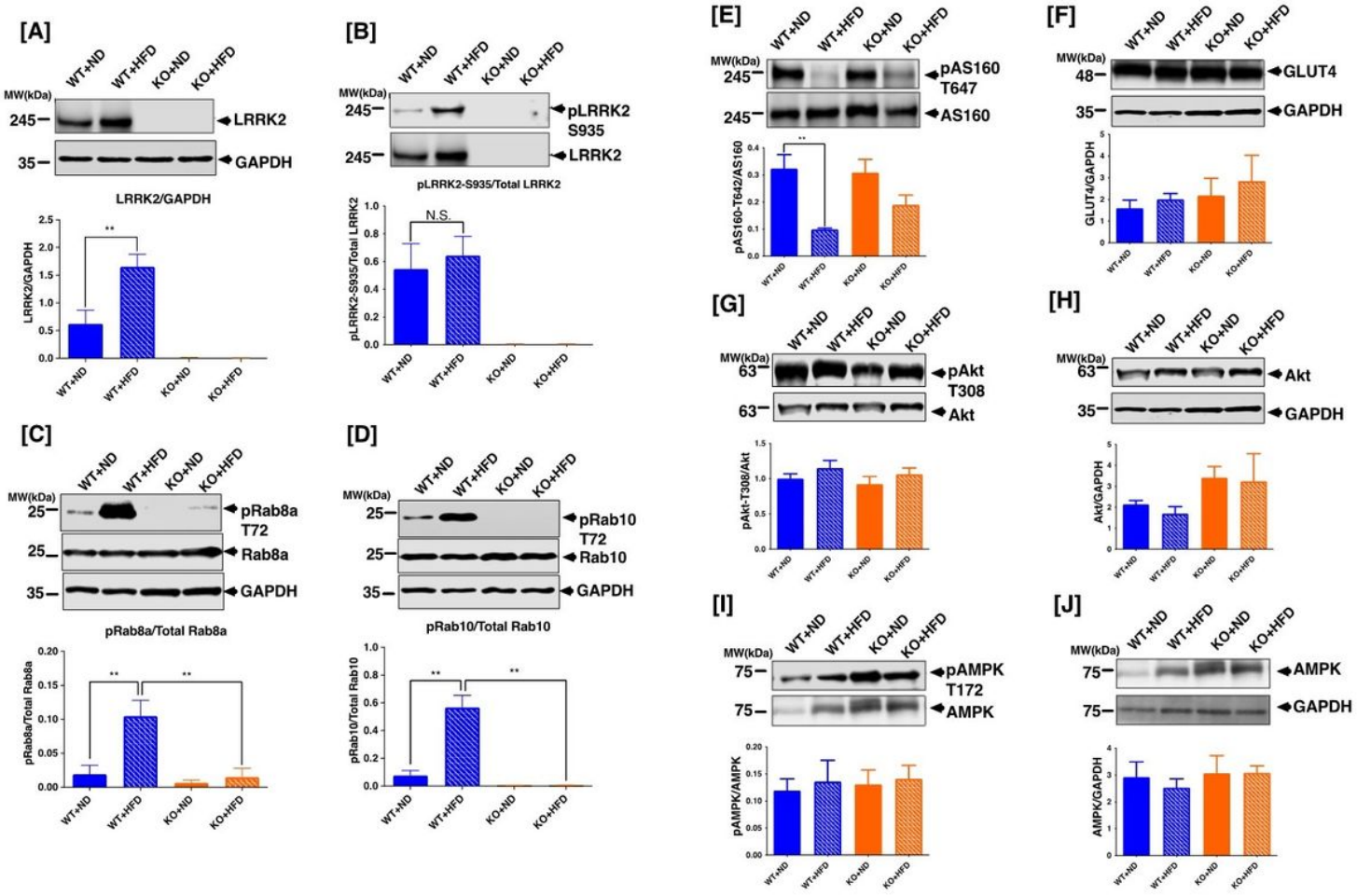

Figure 5

Comparison of protein expression and phosphorylation of Lrrk2, Rab8a and Rab10 in epididymal adipose tissue of ND- or HFD-fed WT and Lrrk2-KO mice.

The expression of Lrrk2 (A), phospho-Lrrk2-S935 (B), phosphor-Rab8a-Thr72 (C) and phospho-Rab10-Thr73 (D) were determined by western blot analysis. These protein bands were visualized by chemiluminescence and GAPDH (loading control) was detected by fluorescence using a LI-COR's Odyssey

Fc Dual-Mode Imaging System (LI-COR Biosciences, USA). The band intensity of Lrrk2 was normalized by GAPDH. The intensity of phospho-Lrrk2, phosphor-Rab8a and phospho-Rab10 were normalized by their total protein band intensity, respectively. Data are presented as means ± SEM (n = 9). The data were analyzed by one-way ANOVA combined with Tukey's post hoc test. **p<0.01.

Fig. 6.

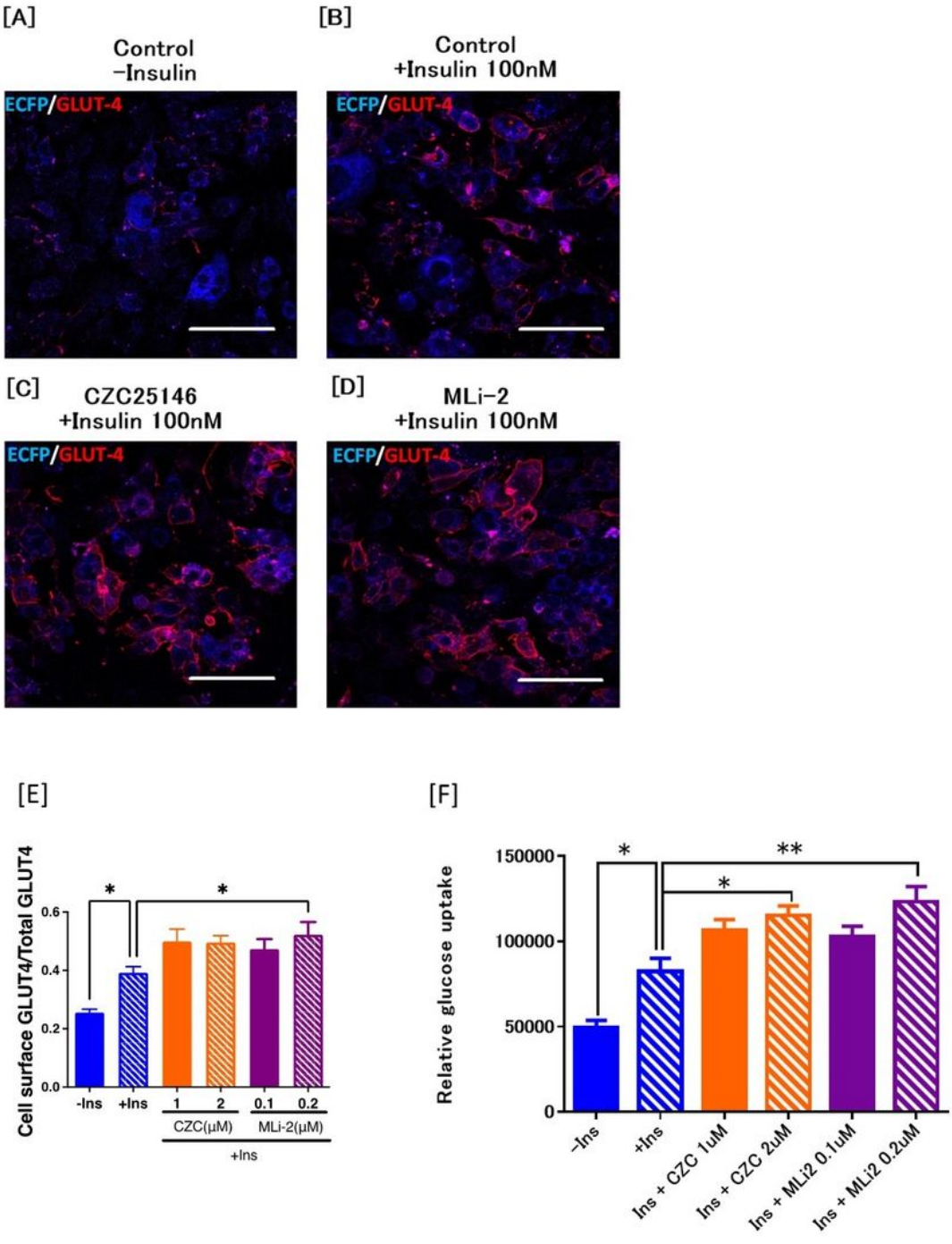

Figure 6

Effect of LRRK2 kinase inhibitor on the GLUT4 membrane translocation in adipocyte and muscle cells.

(A) Differentiated 3T3-L1 adipocytes expressing Myc-GLUT4-ECFP were serum starved and were then treated with or without CZC25146 (2 μM) and MLi-2 (0.2 μM). After that, the cells were stimulated with insulin (100 nM) for 30 min. The cells were then fixed and stained with anti-Myc antibody followed by Alexa594-labeled secondary antibody. Quantification of GLUT4 on the cell surface was performed Image-J software. Data are presented as mean ± SD (n=6). The data were analyzed by one-way ANOVA combined with Tukey's post hoc test. *$p<0.05$.

Fig. 7.

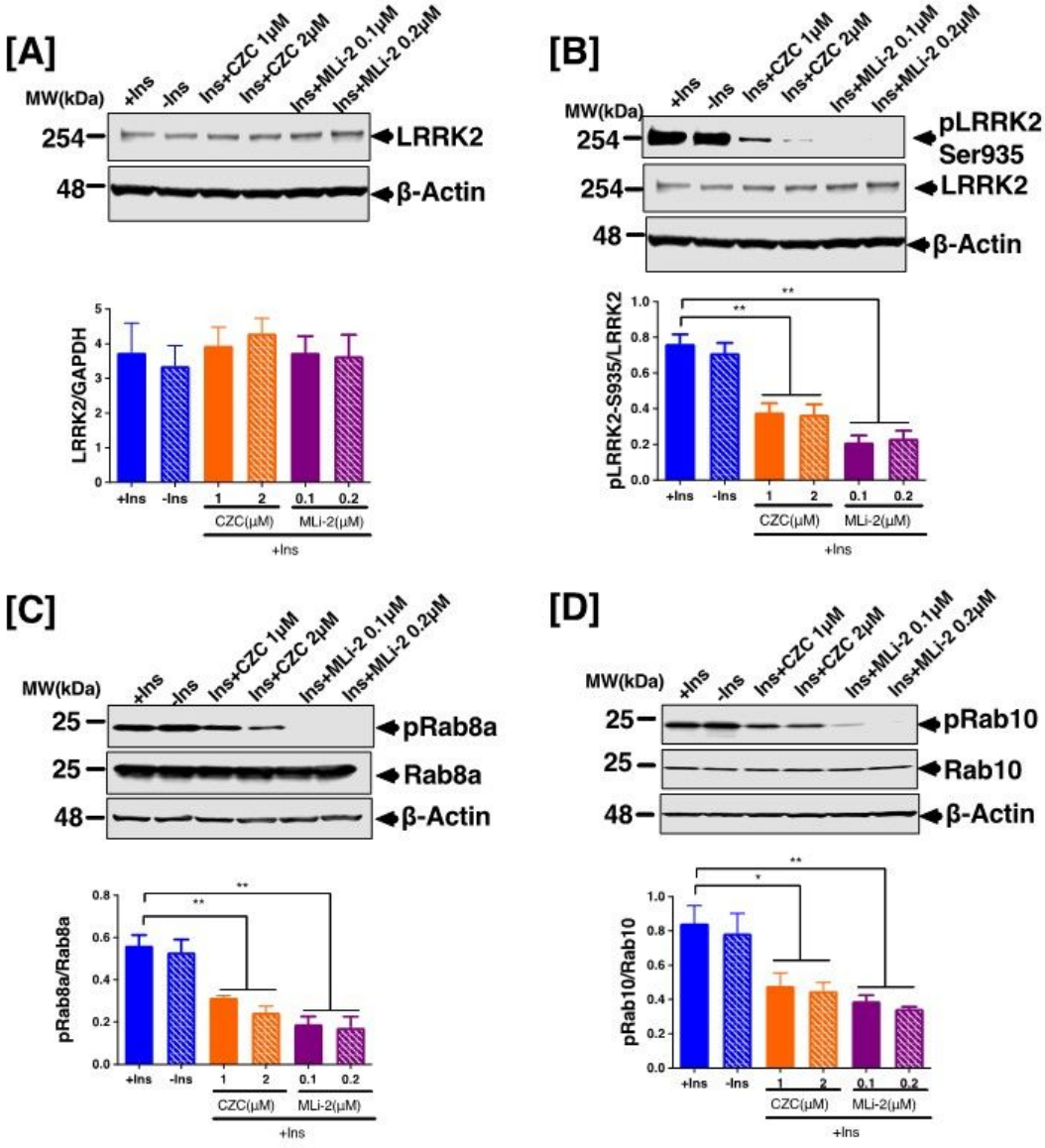

Figure 7

Effect of LRRK2 kinase inhibitor on the phosphorylation of Lrrk2, Rab8a, Rab10, Akt and AMPK in adipocyte and muscle cells.

3T3-L1 cells treated with or without CZC25146 (1 and 2 μM) and MLi-2 (0.1 and 0.2 μM) after serum starved and then stimulated with insulin for 30min. The cells were harvested and analyzed by western

blotting using antibodies against phosphorylated protein such as Lrrk2 (pS935), Rab8a (pT72), Rab10 (pT73), Akt (pS473) and AMPK (pTh172). The expression level of phosphorylated protein was normalized against the total expression level of the target protein. Data are presented as means ± SEM (n = 6). The data were analyzed by one-way ANOVA combined with Tukey's post hoc test. *p<0.05, **p<0.01.

Supplementary Files

This is a list of supplementary files associated with this preprint. Click to download.

- Supplementfigures.pdf
- 2022.10.21.pdf